Static and Flicker Motion Aftereffects in a Velocity Space

Martin J. Wainwright and Patrick Cavanagh
Vision Sciences Lab, Harvard University
33 Kirkland Street, Cambridge, MA 02138
e-mail: {martin, patrick}@wjh.harvard.edu

July 25, 1998

Abstract

Qualitative differences between the static and flicker motion aftereffects (MAEs) have led to several claims that these two MAEs originate at different sites in the visual system. In this paper, we provide evidence for a common site underlying these two effects. In a series of two experiments, we first demonstrate stimuli that yield strong flicker MAEs, but little or no static MAEs. We then develop a stimulus with the opposite effect: it generates a static MAE with little or no flicker MAE. Contrary to a hypothesis of anatomically distinct sites, we show that this dissociation can be explained by assuming only a single site of adaptation within an array of velocity-tuned cells. Our proposal is also consistent with a number of other differences between the static and flicker MAEs.
Keywords: Motion; adaptation; velocity; static; flicker.

Introduction

After prolonged viewing of a moving stimulus, subjects often perceive illusory motion in a subsequently presented test stimulus. This phenomenon, known as the motion aftereffect (MAE), can be measured with either a static test pattern (e.g., a stationary sine wave grating), or a flickering test pattern (e.g., a counterphasing sine wave grating). Recently, it has been reported that the properties of the flicker MAE differ from those of the static MAE [1, 2, 3, 4, 5]. Among these properties are differences in spatial frequency selectivity [6, 1], storage properties [5], and adaptation to first-order compared to second-order stimuli [4]. Such differences have motivated the proposal that the two types of MAE stem from adaptation at different sites in the visual system.

In this report, we begin by providing preliminary evidence against this hypothesis of multiple sites of adaptation. Viewing these test types in a Fourier space of temporal versus spatial frequency clarifies that the two types of aftereffect differ only in terms of the temporal frequency of the test stimulus. Thus, the static and flicker tests can be placed at different points on the same continuum. On the basis of this intuition, we seek experimental evidence for a common mechanism. Our approach is indirect, in that we begin by demonstrating a new dissociation between the static and flicker MAEs. Specifically, in a first experiment, we show a number of first-order motion stimuli that produce a strong flicker MAE with little or no static MAE, whereas the second experiment examines a stimulus with the opposite effect: it generates a static MAE with little or no flicker MAE. According to the usual dissociation

approach, this result would be evidence for the hypothesis of separate sites of adaptation. However, contrary to such logic, we propose that it is not necessary to assume anatomically separate sites of adaptation in order to explain these results. Rather, it is sufficient to consider a *single* site of adaptation in an array of velocity-tuned cells. Therefore, our results provide evidence for a single site of adaptation underlying both the static and flicker MAE, as well as for the role of velocity-tuned units in motion adaptation.

Background

We begin with a brief overview of the standard Fourier space in which the adapting and test stimuli will be analyzed. A standard adapting stimulus is a luminance sine wave grating, described as a function of one spatial variable x, and time t:

$$S(x,t) = M\{1 + C\sin(fx + \omega t)\} \tag{1}$$

where M is the mean luminance, and $C \in [0,1]$ is the Michelson contrast. The luminance is sinusoidally modulated with spatial frequency f and the wave travels at temporal frequency ω. It is useful to view this stimulus in the Fourier space of temporal frequency ω versus spatial frequency f. A sine wave grating of spatial frequency f and temporal frequency ω has a very simple representation in such a Fourier space [7], consisting of two points positioned at (f,ω) and $(-f,-\omega)$, as shown in Figure 1. The velocity $v = -\frac{\omega}{f}$ of the grating is given by the negative slope of the line linking the two points in this Fourier space.

The static MAE is tested using a stationary sine wave grating, meaning that $\omega_{test} = 0$. (I.e. substitute $\omega = 0$ into equation 1 above). In this case, the Fourier spectrum consists of the two points $(f,0)$ and $(-f,0)$ falling on the f-axis, as shown in with open circles in Figure 2. The flicker MAE is often tested with a counterphasing sine wave grating, described by:

$$P(x,t) = M\{1 + C\sin(fx)\cos(\omega_{test}\, t)\} \tag{2}$$

Applying a trigonometric identity yields an equivalent form for this equation

$$P(x,t) = M\left\{1 + \frac{C}{2}[\sin(fx + \omega_{test}\, t) + \sin(fx - \omega_{test}\, t)]\right\} \tag{3}$$

which reveals that a counterphasing grating is the sum of two gratings of the same spatial frequency f, each of half the contrast, and moving in opposite directions (i.e., with temporal frequencies ω_{test} and $-\omega_{test}$ respectively). The Fourier spectrum of such a counterphasing stimulus consists of four points: (f,ω_{test}) and $(-f,-\omega_{test})$ for the one component, with $(f,-\omega_{test})$ and $(-f,\omega_{test})$ for the other component, also plotted with solid squares in Figure 2.

This Fourier space representation shows that the static test is a special case of the flicker test, in which the temporal frequency ω_{test} is equal to zero. That is, the static test falls at one extreme of the continuum of temporal frequency of the test pattern. Such an underlying continuum hints that both types of aftereffect could be viewed within a single framework.

We begin the empirical work with two stimuli that we label the *Wedge* and *Grids* stimuli, both of which yield robust flicker MAEs, but neither of which produces a static MAE. In the second experiment, we complete the dissociation by developing a stimulus that produces a static MAE, but no flicker MAE. In the Theory section, we describe a framework that explains

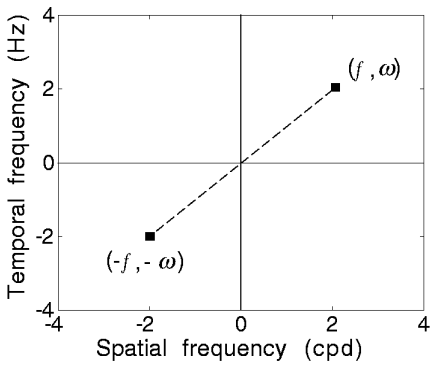

Figure 1: The stimulus is a sine wave of spatial frequency f and temporal frequency ω. In the Fourier space of temporal versus spatial frequency, its amplitude spectrum consists of two points, located at (f, ω) and $(-f, -\omega)$. The negative slope of the dotted line connecting these two point (not actually part of the spectrum) is the velocity v, given by $-\frac{\omega}{f}$.

these results. The combination of the results and the proposed model supports the hypothesis of a common mechanism for both static and flicker MAEs, as well as the role of velocity units in motion adaptation.

Experiment 1: Flicker MAE without Static MAE

In this first experiment, we begin by showing that the *Wedge* and *Grids* stimuli (see Figure 3) produce a robust flicker MAE, accompanied by little or no static MAE. Di Lollo and Bishof [8] have previously reported that a pattern similar to the Grids stimulus used here suppresses the static MAE. Here we confirm this suppression of the static MAE, and moreover we show that the flicker MAE remains intact for both the Grids and Wedge stimuli. We propose that the spatiotemporal Fourier spectra of Wedge and Grids are important in causing this pattern of aftereffects. We then substantiate this claim by showing that the *Fourier component* stimulus,

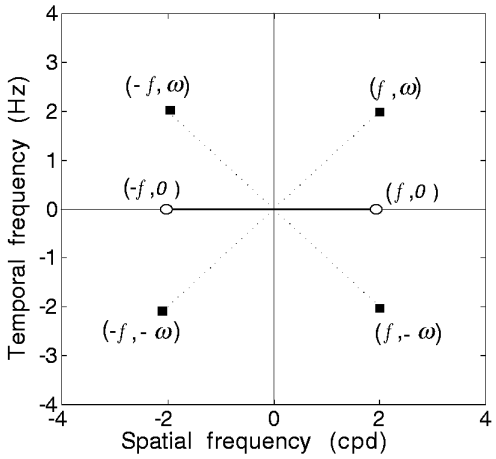

Figure 2: The static test stimulus has a Fourier spectrum consisting of points at $(f, 0)$ and $(-f, 0)$, which are marked with open circles. The flicker MAE is tested with a counterphasing stimulus, which consists of two gratings of equal spatial frequencies f, but opposite temporal frequencies ω and $-\omega$. Thus, the Fourier spectrum of the counterphasing stimulus consists of the four other points shown in solid squares.

which consists of the first three Fourier components of Wedge, also induces a flicker MAE with no static MAE.

Methods

Stimuli:
Adapting and test stimuli were radial gratings, presented within an annulus of inner and outer radii of 1.84° and 5.51° of visual angle respectively. Stimuli were viewed from 57 cm, and viewing distance and stability were maintained with a chin rest. The following four types of stimuli were used.

- The *Standard* stimulus consisted of 6 cycles of a radial sine grating at 40% contrast travelling at 1 Hz. The linear spatial frequency of this grating varied from 0.52 cycles/° at the inner radius of the annulus, to 0.17 cycles/° at the outer radius.

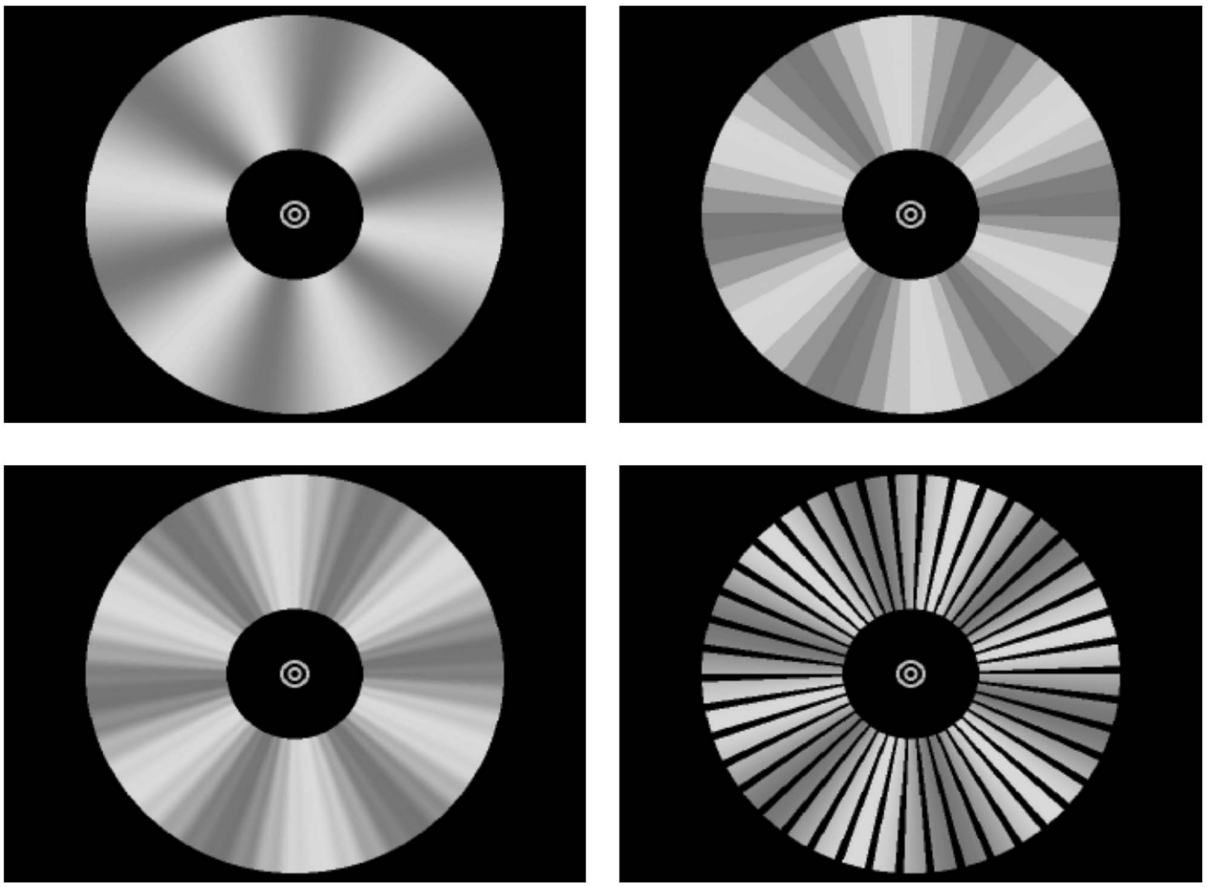

Figure 3: Shown clockwise from the upper left are the Standard, Wedge, Grids, and Fourier stimuli.

- Sampling the standard grating in space generates a characteristic pattern of luminance wedges in space-time; the resulting stimulus is called the *Wedge* stimulus. This spatial sampling induces aliasing, which introduces higher spatial frequency components moving in the opposite direction to the fundamental component. As a result, the Fourier spectrum of Wedge consists not only of the fundamental frequency f moving in one direction, but it also contains gratings of higher spatial frequencies moving in the opposite direction. In particular, when the Wedge stimulus is made by 8 samples per cycle of the standard grating, it can be shown (see Appendix) that the first three components of the Fourier spectrum of Wedge are:

  1. the fundamental frequency: a grating with radial frequency 6 cycles and temporal frequency $\omega = 1$ Hz. (i.e., moving to the left)
  2. a grating with $\frac{1}{7}$ the contrast of the fundamental, and seven times the radial frequency (i.e., $7 \times 6 = 42$ cycles), and temporal frequency $\omega = -1$ Hz (i.e., moving to the right)
  3. a grating of $\frac{1}{9}$ the contrast, 9 times the radial frequency ($9 \times 6 = 54$ cycles), and temporal frequency $\omega = 1$ Hz (moving to the left).

- the *Fourier component* stimulus was the sum of the first three components of Wedge, as described above and shown in Figure 4.

- the *Grids* stimulus consisted of the standard stimulus moving at temporal frequency $\omega = 1$ Hz underneath a grid of black overlaid spokes (i.e. radial lines). Overlaying these black spokes also generates Fourier components of higher spatial frequencies moving in different directions at the same temporal frequency (see Appendix). As a result, the Fourier amplitude spectrum of the Grid stimulus is similar to that of Wedge.

Apparatus
Stimuli were generated with a Power Macintosh 7500/100, and displayed on an Apple high resolution monitor refreshed at 66.7 Hz. The monitor was gamma-corrected using a look-up table.

Subjects
The first author (MW) and one other observer (CM), naive as to the purpose of the experiment, participated in this experiment. Both observers had normal or corrected to normal acuity and were experienced psychophysical observers.

Procedure
In each trial, one type of adapting stimulus, chosen randomly from the four spatial profiles described above, was presented. Direction of movement alternated between clockwise (CW) and counterclockwise (CCW) on each trial. While fixating the central bull's-eye, observers viewed the adapting stimulus for 30 seconds. After this adaptation period, the test stimulus was presented, and observers reported the perceived direction of motion for 30 seconds by pressing and holding down one key for CW motion, and another key for CCW motion. The static MAE was measured with the standard stimulus presented at 40% contrast and 0 Hz, whereas the flicker MAE was tested with a standard grating of 40% contrast counterphasing at

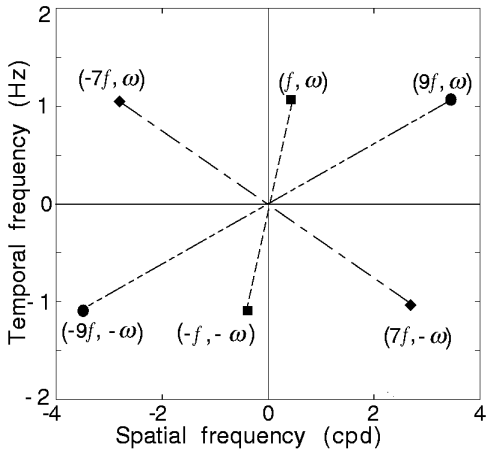

Figure 4: Shown are the first three Fourier components of the *Wedge* stimulus: the fundamental at (f, ω) with squares, the first harmonic component at $(7f, -\omega)$ with diamonds, and the second harmonic component at $(9f, \omega)$ with circles. The *Fourier* stimulus is formed as a linear sum of these first three Fourier components.

1 Hz. This procedure yielded reliable measurements of MAE duration. At least two minutes were taken off between trials to ensure that adaptation to the previous trial had completely faded.

Results

The durations of static and flicker MAEs are shown for both observers in Figure 5. Both observers reported moderate static MAEs ($\approx$ 5s) for the standard adapting stimulus (solitary bar in top row graphs), and no static MAE whatsoever (0 s reported in all trials) for the Wedge and Grids pattern. One possibility is that the Wedge and Grids stimuli produce no static MAE due to interference from the higher frequency components, and in particular those moving in direction opposite to the fundamental frequency. To test this hypothesis, we also measured the static and flicker MAEs for the Fourier stimulus composed of the first three

Fourier components of Wedge. Consistent with this proposal, observers reported little or no static MAE following adaptation to the Fourier component stimulus.

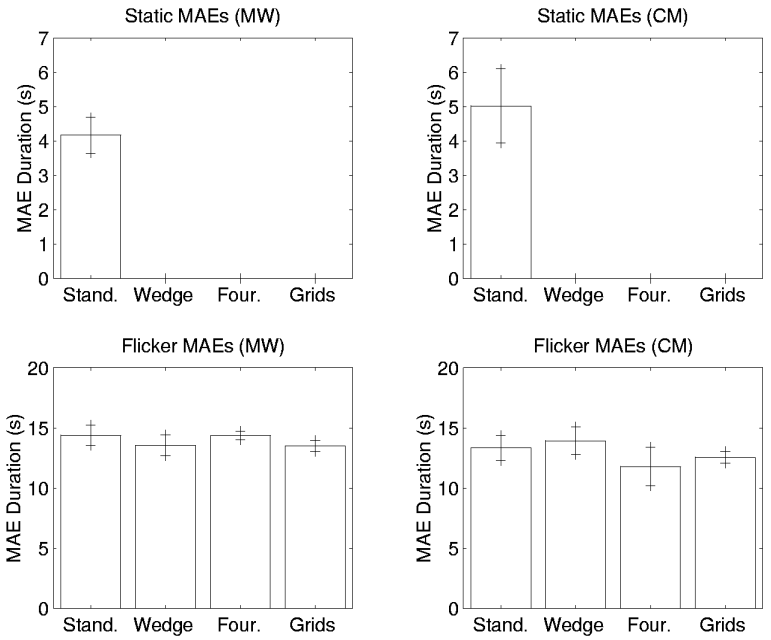

Figure 5: Durations of static MAEs (top row) and flicker MAEs (bottow row) for observers MW (left column) and CM (right column). No static MAEs were ever reported for any of the Wedge, Grids, or Fourier stimuli. Error bars shown are $\pm$ standard errors of the mean.

Although they did not produce a static MAE, both the Wedge and Grid stimulus produced strong flicker MAEs (13-15s), of a strength comparable to the flicker MAE produced by the Standard stimulus. Similarly, the Fourier stimulus yielded a strong flicker MAE, again comparable to that produced by the standard stimulus.

Discussion

Three aspects of this data are worthy of remark. First of all, the results of this experiment clear up a pair of minor unresolved questions. Di Lollo and Bischof [8] first reported that the Grids stimulus completely suppressed the static MAE, but did not provide an explanation. The results of the current experiments show that the static MAE is suppressed by the presence of higher spatial frequency components moving in the opposite direction. Furthermore, Di Lollo and Bischof [8] reported weaker static MAEs with temporally sampled square wave gratings as opposed to sine waves. These reduced aftereffects can also be explained by again taking

into account the effects of sampling, which is in this case temporal rather than spatial. (See General Discussion for issues of temporal sampling in the context of Nishida and Sato [4].)

The second point of interest concerns interaction across large spatial frequency differences. Recall that the spatial frequency of the first harmonic component in the Fourier pattern is seven times higher than the fundamental component. Therefore, the suppression of the static MAE is interesting, because it reveals interactions across spatial frequencies separated by nearly three octaves. Such large differences in spatial frequency are far beyond most psychophysical estimates of channel bandwidths, which are typically between 1 and 2 octaves [9, 10, 11, 12]. We will return to the significance of this interaction across such a large difference in spatial frequency during the subsequent theoretical development.

Thirdly, the results of this experiment present an intriguing dilemma. Specifically, why is it that higher frequency components moving in the opposite direction suppress the static MAE, yet do not affect the flicker MAE? One possibility is that the flicker MAE is simply a more sensitive measure of adaptation [4], so that a flickering test reveals adaptation despite some interference from higher frequency components. We address this possibility in the following experiment.

Experiment 2: Static MAE without Flicker MAE

This second experiment serves to eliminate the hypothesis that the flicker MAE is a more sensitive measure than the static MAE. In order to do so, we develop a stimulus that produces a static MAE, while producing little or no flicker MAE. Details of the theory underlying the development of this stimulus are given in the Theory section. This experimental result thus completes the double dissociation between the flicker and static MAEs.

Methods

Stimuli

Stimuli were presented within two rectangular boxes ($5.51° \times 9.18°$) offset above and below the central bull's-eye by $0.73°$. Within each of these boxes, stimuli travelled in opposite directions in order to minimize optokinetic nystagmus. Stimuli were viewed from 57 cm, with head position maintained using a chin rest. Adapting stimuli were of the following two types:

- the *Base* stimulus was a linear grating of spatial frequency 0.50 cycles/° and 40% contrast moving with temporal frequency 0.50 Hz.
- the *Compound* stimulus consisted of the Base stimulus (moving in one direction) superimposed upon a second linear grating of 40% contrast, spatial frequency 0.25 cycles/° with temporal frequency 0.75 Hz (moving in the opposite direction).

Subjects

The first author (MW), and a second observer (AH), naive as to the experimental purpose, participated in this study. Both observers had normal or corrected to normal acuity, and were experienced psychophysical observers.

Procedure

On any given trial, one type of adapting stimulus, chosen randomly from the two spatial

profiles described above, was presented. The direction of movement alternated on each trial. While fixating the central bull's-eye, observers viewed the adapting stimulus for 30 seconds. During the test phase, the lower box was blanked out, and the test stimulus was presented alone in the upper box. This arrangement was designed to eliminate possible interference between the two boxes during measurement of the aftereffects. During the test period, observers reported the perceived direction of motion for 30 seconds by pressing and holding down one key for leftward (L) motion, and another key for rightward (R) motion. The static MAE was measured with the Base grating (0.50 cycles/°) presented at 40% contrast and 0 Hz, whereas the flicker MAE was tested with the same grating counterphasing at either 1 Hz or 2 Hz. At least two minutes were taken off between trials to ensure that adaptation to the previous trial had completely faded.

Results and Discussion

Presented in Figure 6 are the durations of the static and flicker MAEs for subjects MW and AH. For both subjects, the Compound stimulus yielded little or no flicker MAEs, at both 1 Hz and 2 Hz. On the other hand, the Compound stimulus yielded static MAEs comparable to those of the standard stimulus. These results show that the flicker MAE can be suppressed while preserving the static MAE, thereby ruling out the hypothesis that the flicker MAE is simply more sensitive under all conditions.

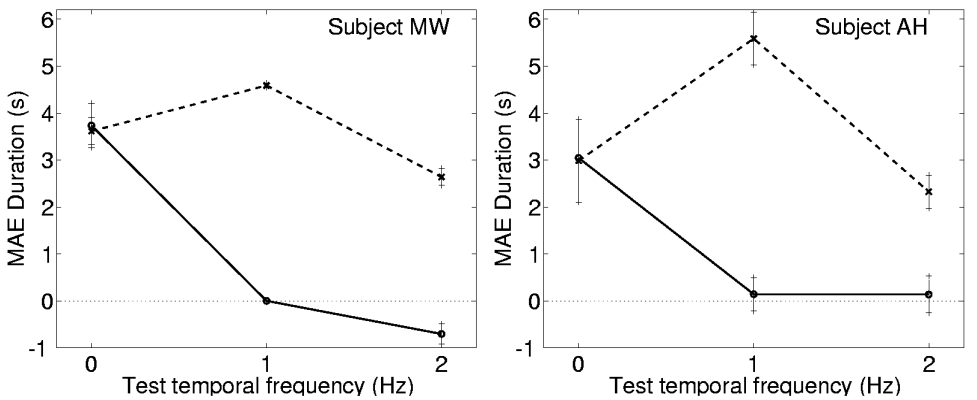

Figure 6: MAE duration for the *Base* stimulus (dotted line) and the *Compound* stimulus (solid line) for observers MW (left) and AH (right). MAEs were measured at 0 Hz (static test), 1 Hz and 2 Hz (both flicker tests). The static MAEs for both tests were of comparable magnitude, whereas the Compound stimulus produced little or no flicker MAE. Error bars shown are $\pm$ standard error of the mean.

With this second experiment, we have completed the double dissociation between the static and flicker MAEs. The Compound stimulus was developed from theoretical grounds for the specific purpose of suppressing the flicker MAE while still producing a static MAE. We now turn to a description of this theoretical basis.

Theory

Two aspects of the data from the previous two experiments are interesting. First of all, we produced a double dissociation between the static and flicker MAEs. That is, on one hand, we exhibited stimuli that produce a robust flicker MAE but no static MAE, while on the other hand, we developed a stimulus with the opposite effect (a static MAE but no flicker MAE). Secondly, the pattern of aftereffects revealed interactions across fairly large differences in spatial frequency. For instance, our data from the first experiment show that the static aftereffect of a grating of spatial frequency f can be suppressed by a grating of $\frac{1}{7}$ the contrast, and seven times the spatial frequency. However, these higher frequency gratings had no effect on the flicker MAE. Therefore, any proposal needs to account for both the interaction across fairly large spatial frequency differences, *as well as* the asymmetry in these interactions.

One possibility, as suggested by other authors [1, 5, 13], is that the static and flicker MAEs stem from separate sites of adaptation in the visual system. We argue that anatomically separate sites are not necessary; instead, we account for our results by postulating only a single site of adaptation. In this framework, velocity — *not* temporal frequency — is the underlying dimension. This choice permits the necessary interactions across differences in spatial frequency, since structures of different spatial frequency content can still move at the same velocity. Other evidence for the role of velocity in motion adaptation is discussed in a subsection on velocity aftereffects in the General Discussion.

Adaptation in a Speed Space

Low-level motion detectors can be modeled as spatiotemporal energy filters that are tuned to a particular spatial and temporal frequency [14]. These quasi- linear filters operate by extracting the oriented bands in space-time that correspond to a rigidly translating object. Equivalently, they are sensitive to local bands of energy in a spatiotemporal Fourier space (see Figures 1 and 2). It is important to note that these kinds of spatiotemporal bandpass filters are *not* velocity- sensitive, but rather are tuned to a particular spatiotemporal frequency. By combining the outputs of a collection of motion energy detectors, it is possible to construct a velocity-tuned unit, and a number of such schemes have been proposed [15, 16, 17].

For simplicity, we consider velocity-tuned units of the form shown in Figure 7, which correspond to the "speed-tuned" units of the form reported by Rodman and Albright [18]. The transition from the earlier Fourier space diagrams (e.g., see Figures 1 and 2) to such a velocity diagram (see Figure 7) can be understood geometrically as follows. In the Fourier space, velocity corresponds to the polar angle on a circle about the origin. So a circle in the Fourier space is mapped onto the horizontal axis in this new co-ordinate system, which corresponds to velocity. Consider a unit tuned to a rightward velocity $v_t > 0$; while it responds optimally to v_t, it will also respond to a stationary stimulus ($v = 0$). This unit is matched with a leftward counterpart, which responds optimally to $-v_t < 0$. In Figures 7, 8, and 9, the response of a leftward unit will be shown as negative for reasons to be discussed shortly. Consistent with other psychophysical dimensions (e.g., spatial frequency), we consider velocity units with tuning widths that scale with their preferred velocity. Thus, the tuning curves of higher velocity units will be broader than the tuning of slower velocity units. This type of tuning can be further justified, depending on the structure of the underlying motion energy

units [16].

Opponency in Motion Detection

As with other models [19, 20], our hypothesis hinges on opponency between different detectors. There are many psychophysical manifestations of opponency between detectors tuned to opposite directions of motion. A straightforward example is a counterphasing grating: although this stimulus consists of two gratings traveling in opposite directions at the same velocity (see equation 3), it is perceived as stationary. That is, rightward and leftward motion signals cancel out one another, suggesting that opposite direction motion channels are linked together in opponent fashion. In general, competition will occur among detectors tuned to all different velocities (directions and speeds). Given that the experimental stimuli in this paper were all one-dimensional, we need here to consider only opponency between detectors that are tuned to the same speed but to opposite directions. It is to represent this fundamental opponency that Figures 7 through 9 depict leftward responses with a negative sign compared to the rightward (positive) responses.

Before turning to adaptation, we highlight a crucial difference between the perception of stationary and counterphasing gratings under non-adapted conditions. In both cases, because of the opponency, motion perception depends on the balance between rightward and leftward responses. When a stationary (zero velocity) grating is presented under normal (non-adapted) circumstances, the rightward response is balanced by an equivalent leftward response. Here, the opponency will involve responses in the neighbourhood of zero velocity. On the other hand, a counterphasing stimulus consists of two gratings of equal spatial frequency traveling in opposite directions (i.e., with velocities v_{test} and $-v_{test}$ respectively). When this stimulus is presented under normal (non-adapted) conditions, the response of channels near to v_{test} balances the response of the opposing channels near to $-v_{test}$. For this reason, despite the substantial motion energy content of the stimulus itself, it generates no net motion signal after the opponency, and it is perceived as being stationary. In this case, the opponency will be between tuned units in neighbourhoods of v_{test} and $-v_{test}$. Consequently, tests of the static and flicker MAE probe different subsets of the velocity-tuned units. This difference between the stationary and counterphasing test will figure prominently in discussion of the experimental results.

Aftereffects with Single Component Stimuli

Neurophysiological data shows that prolonged stimulation of a cell with a moving stimulus causes a decrease in its response [21, 22]. Suppose that the rightward unit responding optimally to velocity v has been adapted in this fashion; then its new depressed response curve is shown by the dotted line in Figure 7. After this adaptation process, a stationary (i.e., with zero velocity) test grating is presented. Many pairs of left/right units (not all shown) will respond to this stationary grating, but because of the inherent opponency, most pairs will signal zero net motion. Only filter pairs in which one direction has been adapted will signal non- zero net motion. Overall, the net response will be leftward, and the truly stationary grating will be perceived to drift slowly to the left. For the flicker MAE, the logic is similar, except that the test stimulus consists of two gratings moving at velocities v_t and $-v_t$. As

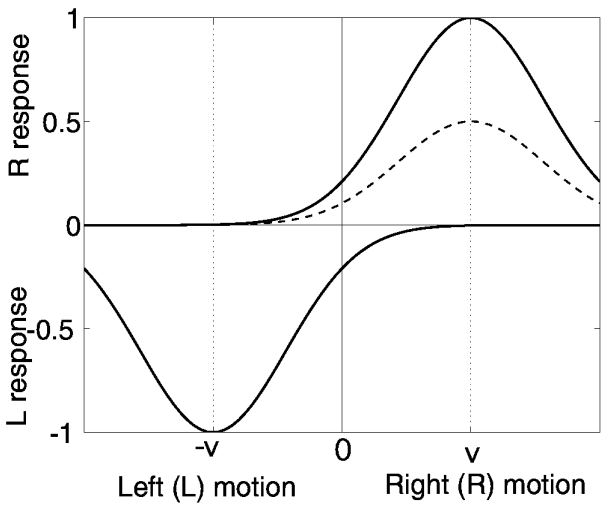

Figure 7: Represented on the horizontal axis is velocity, whereas the vertical axis shows the responses of velocity units. By convention, positive will correspond to rightward motion, whereas negative will correspond to leftward motion. Two channels, sensitive to rightward velocity v_t and leftward velocity $-v_t$, are shown in solid lines. Adaptation of the rightward channel leads to a decrement in its response, indicated by the dotted line underneath the fully-responsive rightward channel. A static MAE is tested by probing at zero velocity, whereas the flicker MAE is tested by comparing responses at velocities in a neighbourhood of v_{test} and $-v_{test}$.

a result, the opponent comparison in this case will be between left/right units in the neighbourhood $-v_t$ and v_t. The (leftward) response around $-v_t$ will be stronger than the adapted (rightward) response around v_t, resulting in a net perception of leftward motion.

Such a proposal for the generation of aftereffects — opponency between different detectors — has been standard for many years (see, for instance, Sutherland [19], or Mather [20]). The novel component of this proposal is that opponency occurs among velocity-tuned units. For this reason, although the logic underlying the static and flicker MAEs are similar, there is an important difference. Since many velocity units show residual sensitivity to stationary stimuli, the static MAE potentially depends on the output of many velocity units. On the other hand, some units tuned to lower velocities will not respond to higher velocities. Due to this high velocity cut-off, some of these units will not play a role in the flicker MAE under certain conditions — namely when their upper cutoff is lower than the velocity of the stimulus used to test the flicker MAE. It is this difference that is crucial in our explanation of the experimental results.

Stimuli with Multiple Components

The stimuli used in the current experiments are slightly more complex, because they consist of multiple spatial frequency components moving at different velocities. For instance, although it is not immediately apparent, recall that even a stimulus like Grids contains Fourier components of higher spatial frequencies moving at various velocities (see Appendix). In the following paragraphs, we outline how the framework described above can account for the experimental results obtained with these more complex adapting stimuli. In short, it is necessary to consider three factors:

- which velocity-tuned units are stimulated (and hence adapted) by the adapting stimulus
- the contrast of the various components in the adapting stimulus, which partly determines the strength of the adaptation
- which velocity-tuned units are tapped by the test stimulus (i.e., whether a static or a flicker test is used). Again, a static test will stimulate all units around zero velocity, whereas with a flicker test, only units tuned to higher velocities will respond.

It is the interaction of these three factors that determines the strength of any motion aftereffect.

Flicker without Static MAE

Consider first the stimuli used in experiment 1. We will show here that the changes in sensitivity following adaptation to the Wedge, Grids or Fourier stimuli are balanced in the velocity units that respond to static tests, but *imbalanced* in units that respond to the higher velocities of the flicker test. The static and flicker test stimuli tap different sub-populations of these velocity units; this difference results in no aftereffect for the static test, but a robust aftereffect for the flicker test.

As discussed earlier, the spatial sampling (at 8 times per cycle) in Wedge introduces a Fourier component (7 times the spatial frequency) moving in the opposite direction at the

same temporal frequency. Consequently, in terms of velocity, the fundamental component of spatial frequency f is moving at some velocity v_{fund}, whereas the first harmonic component is moving at velocity $-v_{first} = -\frac{1}{7}v_{fund}$ (that is, in the opposite direction). We consider the velocities of these components in the framework described above. Figure 8 shows units responding optimally to $\pm v_{first}$ in solid blue lines, as well as other units responding optimally to the higher velocity $\pm v_{fund}$ in solid red lines. Observe that again that all channels respond somewhat to stationary ($v = 0$) stimuli. To a first approximation, adapting to a rightward-moving Wedge stimulus will result in adaptation of the v_{fund} unit (rightward motion), as well as the $-v_{first}$ unit (leftward motion). Following adaptation, these adapted units will give weaker responses than normal, as is shown by the dotted lines underneath the v_{fund} and $-v_{first}$ response curves. Observe that the decrement in the v_{fund} channel is greater than that in the v_{first} channel, because the contrast of the spatial frequency component stimulating the v_{fund} channel is greater than the component stimulating the v_{first} channel. In order to measure a static MAE, a stationary (zero velocity) grating is presented. On one hand, the $\pm v_{fund}$ pair will signal net leftward motion (because the rightward unit is adapted); on the other hand, the $\pm v_{first}$ pair will signal net rightward motion (because the leftward unit is adapted). Thus, the critical comparison is between the leftward signal of the v_{fund} pair versus the rightward signal of the v_{first} pair. Note that there are two factors that trade off against one another. Although the depression in the v_{fund} channel is greater overall (due to higher contrast), the v_{fund} response drops off at zero velocity. On the other hand, the v_{first} channel, being tuned to a lower velocity overall, retains a stronger response at zero velocity. Consequently, although the overall decrement in the v_{first} channel is weaker, it is "read-out" more strongly at zero velocity than the stronger adaptation in the v_{fund} channel. In this way, consistent with empirical observations, these leftward and rightward motion signals should cancel, resulting in a net zero motion signal, and hence no static MAE from the Wedge stimulus.

Now consider the flicker MAE test, using a counterphasing stimulus that consists of two gratings moving in opposite directions at velocities $\pm v_{test}$. In this example $v_{test} = v_{fund}$. For this test stimulus, the relevant comparison will be between units responding to $\pm v_{fund}$. As with the static test, the $\pm v_{fund}$ pair will signal net leftward motion, because the rightward unit is adapted. However, in this situation, the $\pm v_{first}$ pair is not stimulated by the $\pm v_{test}$ counterphasing stimulus, due to the relatively sharp drop-off in its velocity response function (note that the blue lines of the $\pm v_{first}$ responses in Figure 8 are effectively zero at $\pm v_{fund}$). Consequently, unlike with the static test, there will be little or no interaction between the $\pm v_{first}$ and $\pm v_{fund}$ pairs in the flicker MAE test. Rather, the $\pm v_{fund}$ pair will signal leftward motion, and, again consistent with empirical observation, a leftward flicker MAE for the Wedge stimulus will result.

Thus, the proposed framework accounts for the presence of a flicker MAE but absence of a static MAE for the Wedge stimulus. The key factor was that the static and flicker MAE tests probe different subsets of the velocity units. A similar rationale applies to both the Grids and Fourier component stimuli, due to the fact that they also contain components moving in opposite directions at different speeds.

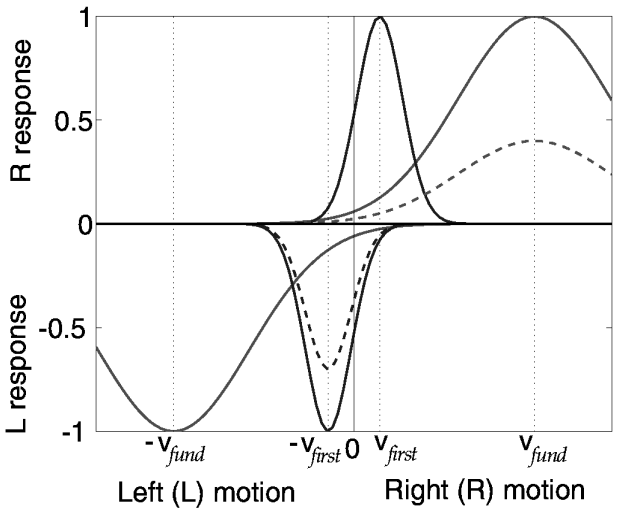

Figure 8: Two units responding optimally to velocities $-v_{fund}$ and v_{fund} (leftward and rightward respectively) are drawn in solid red lines. Two other units tuned to $\pm v_{first}$ are drawn in solid blue lines. The Wedge stimulus causes adaptation in the $+v_{fund}$ and $-v_{first}$ units, causing a decrement in their response. These decreased responses are shown in dotted lines below the full response curves. The static MAE is tested at velocity 0, whereas the the flicker MAE taps into units at velocities $-v_{fund}$ and $+v_{fund}$, corresponding to the sine waves in the counterphasing test stimulus. See text for more details.

Static without Flicker MAE

The second experiment involved the Compound stimulus, which produced a static MAE but little or no flicker MAE. This compound stimulus was explicitly designed so that changes in sensitivity following adaptation would be balanced for the flicker test, but *imbalanced* for the static test. Here we examine how the changes in sensitivity were arranged to be different for the two types of test.

The compound stimulus consisted of one grating moving at velocity $-v_{2f}$ (leftwards), and the other moving at velocity $v_f = 3\,v_{2f}$ (rightwards). These channels and their velocity response curves are depicted in Figure 9. Adapting to the Compound stimulus will depress both the leftward $-v_{2f}$ and rightward v_f channels. The adapted responses for the $-v_{2f}$ and v_f units are shown in dotted blue and red lines respectively. In this case, the size of the decrements will be roughly comparable, because the contrasts of the two adapting components were set equal at 40%. As usual, the static MAE is measured with a stationary test grating ($v_{test} = 0$). The high contrast grating moving at velocity $-v_{2f}$ to the left will strongly adapt the $-v_{2f}$ channel; as a result, the v_{2f} pair will provide a net strong rightward signal when tested at zero velocity (see the zero velocity line in Figure 9). Although the $-v_f$ channel will also have been adapted, the effect of this adaptation will not be as strong at zero velocity because the $-v_f$ response drops off more strongly towards zero. At the zero velocity point, the strong rightward signal of the $\pm v_{2f}$ pair will overpower any weaker leftward signal from the $\pm v_f$ pair. Consequently, a rightward static MAE should result, as was empirically observed.

It is important to contrast this interaction — between the v_f and v_{2f} channels — with the v_{fund} / v_{first} interaction involved in first experiment. In both cases, two factors play off against one another: the strength of the decrement (adaptation) in the channel, and the drop-off in the channel towards zero velocity. In the latter case, although the v_{fund} channel was more strongly adapted (higher contrast grating) than the v_{first} channel, it also dropped off more strongly towards zero. Thus, the decrements in both channels tended to be of equal strength, and to cancel one another. On the other hand, in the v_f / v_{2f} case just described, both channels were equally adapted, because gratings of equal (40%) contrast were chosen. In this case, given the greater drop-off in the v_f channel, the v_{2f} decrement will dominate at zero velocity.

Continuing with the results of the second experiment, we first consider the flicker MAE tested with a $2f$ counterphasing grating at 1 Hz, which corresponds to a velocity $v_t = 2\,v_{2f}$. Note that $v_{2f} < v_t = 2\,v_{2f} < v_f = 3v_{2f}$, so that the adapted channels fall on either side of the test velocity. In addition, the contrasts of the f and $2f$ gratings are equal, so the degree of adaptation in the $-v_{2f}$ unit (leftward) will be roughly equivalent to the adaptation in the v_f unit (rightward). Therefore, the two contributions of these two units will be roughly equal, and so cancel one another out. In Figure 9, this cancellation is seen by observing that the decrement in the $-v_{2f}$ unit (difference between solid blue and dotted blue curves) at $-v_{test}$ is roughly equal to the decrement in the v_f channel (difference between the solid red and dotted red curves) at the test velocity v_{test}. A flicker MAE depends on an imbalance between the leftward motion signals at $-v_{test}$ and the rightward motion signals at v_{test}. Here, the lack of such an imbalance at v_{test} means that no flicker MAE should occur, as was documented in Experiment 2.

As for the flicker MAE tested at 2 Hz, the test velocity in this case falls closer to the

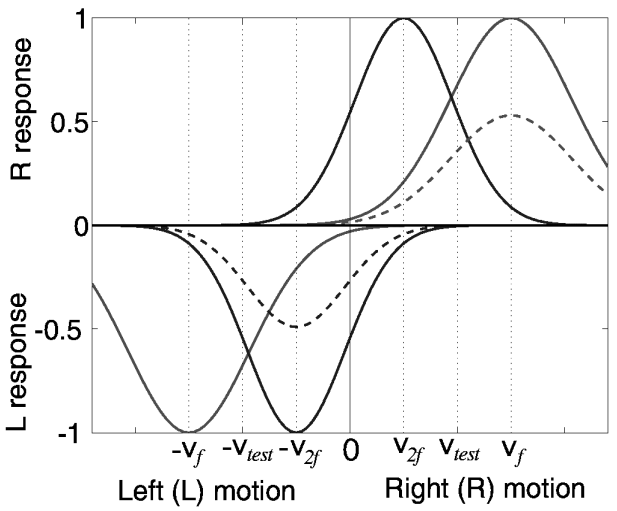

Figure 9: Two units responding optimally to velocities $-v_{2f}$ and v_{2f} (leftward and rightward respectively) are drawn in solid blue lines. Two other units tuned to $\pm v_f$ are drawn in solid red lines. The compound stimulus in Experiment 2 causes adaptation in the $-v_{2f}$ and $+v_f$ units, causing the depressed response curves drawn in dotted lines, below the full- response curves. The static MAE is tested at zero velocity, whereas the flicker MAE is tested at the tested velocities v_{test} and $-v_{test}$.

v_f channel, meaning that one might expect an aftereffect in the opposite direction. A weak reversal was seen in the 2 Hz test in Experiment 2 for one of the two subjects. According to the current account, this feature of the compound stimulus — namely, that the velocities of the two components are relatively well-balanced around the test velocity – should be critical to ensure that no flicker aftereffect is generated. Therefore, if the current account is correct, then by changing the balance between the adapting and test velocity, it ought to be possible to systematically reverse the direction of the flicker MAE. One way to disrupt this balance is to change the velocity of one of the components forming the compound stimulus. In order to test our account, we varied the velocity of one component in such a compound stimulus, and measured the flicker MAE at 1 Hz for various velocities of the component. The results revealed the systematic reversal that is expected, in which the direction of the flicker MAE changed systematically from leftward to rightward.

General Discussion

Other Differences

Previous authors have argued that qualitative differences between the static and flicker MAEs support the hypothesis of anatomically distinct sites of adaptation. The general idea is that the properties of the static MAE are more consistent with adaptation at an "earlier" level (e.g. V1), whereas the flicker MAE is more consistent with "higher" processing (e.g. MT). In the current work, we have produced a new double dissociation between the static and flicker MAEs. Although our results could be interpreted as further evidence for anatomically distinct sites, we have proposed that they can be understood in a velocity space. Our "separate sites" are in fact different sub-populations of velocity-tuned units that underlie the two kinds of aftereffects. These units all respond in an analogous fashion, albeit with different preferred velocities, and are likely to be located at the same anatomical site. In this section, we review some of these differences cited in support of anatomically distinct sites of adaptation, and argue that many of them are consistent with the current proposal of aftereffects in a velocity space.

Storage Differences

It has been reported that the static and flicker MAEs differ in terms of their storage properties. Specifically, Verstraten et al. [5] used moving random pixel arrays to test for storage of the static MAE following a dynamic test, and vice versa. They found an interesting phenomenon: whereas the static MAE shows almost complete storage following a dynamic test, the flicker MAE shows no or very little storage following a static test. Although such a result could be interpreted as evidence for multiple sites, we find that it can also be understood within the current proposal by considering the following two factors.

First of all, our model consists of an array of velocity-tuned units, such that *(a)* each unit shows at least some sensitivity to stationary (zero velocity) patterns, but *(b)* units tuned to lower velocities cut off earlier than units tuned to higher velocities. (See Figure 7). The static MAE is determined by a comparison between rightward and leftward responses at zero velocity, whereas the flicker MAE tested at velocity v_{test} is determined by comparing

the responses of units around $v_{test} > 0$ to those around $-v_{test} < 0$. Therefore, a key difference is that although testing a static MAE will necessarily involve probing those units that determine the flicker MAE, the converse statement *does not* follow. That is, testing a flicker MAE does not necessarily probe all the units involved in the static MAE: in particular, units tuned to sufficiently low velocities will not be (strongly) stimulated by a given dynamic test.

Secondly, MAE decay is slowed down when no test stimulus is present after adaptation [23]. This observation shows that MAE decay depends upon stimulation of the underlying units that determine the aftereffect. In other words, MAE storage occurs when the units underlying the aftereffect are not stimulated during the storage period. The fact that MAE duration decreases with increasing test contrast [24] also supports this idea of MAE storage depending on how strongly (if at all) the underlying units are stimulated.

On the basis of these two factors, we predict that because a static MAE test will stimulate those units involved in the dynamic MAE, any sort of adaptation should decay during a static test. Therefore, no or little storage of the dynamic MAE should be observed following a static test. In contrast, since testing a dynamic MAE will *not* stimulate all units involved in a static MAE, storage of the static MAE could be observed following a dynamic test, depending on the temporal structure of the dynamic test (see next paragraph). It is precisely this pattern of results that was reported by Verstraten et al. [5], as described above.

Furthermore, we can make a secondary prediction about how the amount of static MAE storage should vary as a function of the temporal structure of the preceding dynamic test. In particular, because dynamic tests at higher velocities (higher temporal frequencies) will stimulate and thereby "re-adapt" *fewer* of the units involved in the static MAE, it follows that static MAE storage should be greater following dynamic tests that involve higher temporal frequencies (higher velocities). This pattern shows up in the data of Verstraten et al. ([5]; see Figure 2), where all three subjects report more storage of the static MAE following a 90 Hz dynamic test compared to storage following a 10 Hz dynamic test.

Spatial Frequency Selectivity

Cameron et al. [6] used a tracking procedure to measure the velocity of static MAEs. Consistent with earlier work [25], they found that the static MAE was selective for spatial frequency, meaning that the maximal aftereffect occurred when the spatial frequencies of the adapting and test gratings were equal. Using MAE duration as the measure, Ashida and Osaka [1] replicated this result for the static MAE. Furthermore, they reported relatively little spatial frequency selectivity for a flicker test at 5 Hz. In subsequent work, Bex et al. [26] showed that any difference between the static and flicker MAEs is *graded* rather than absolute. Specifically, measuring MAE durations for a 0.25 Hz test, Bex et al. showed that the flicker MAE is also selective for spatial frequency.

First of all, the overall trend of these results is consistent with the current proposal. Specifically, the data show a clear continuum from the lower extreme of the static MAE (0 Hz), through low temporal frequency flicker MAEs (0.25-1 Hz) and onto the upper extreme of higher temporal frequency (5 Hz) flicker MAEs. Secondly, the specifics of the results are also plausible given known features of the tuned spatial and temporal channels that underlie velocity coding [27]. For example, it is known that spatial tuning at higher temporal frequencies

is broader [28]. (Note that this behavior supports our choice of broader velocity tuning for higher velocities). As we have argued, the static MAE is determined by comparisons among units tuned to low temporal frequencies (velocities), whereas the flicker MAE is determined by opponent comparisons among units tuned to higher temporal frequencies (velocities). If units at higher temporal frequencies are more broadly tuned to spatial frequency, then the flicker MAE tested at high temporal frequencies should show less spatial frequency selectivity.

First versus second-order motion?

Another cited difference between flicker and static MAEs is their behavior with first- compared to second-order motion. According to current proposal, certain differences between static and flicker MAEs following adaptation to second-order motion might be understood by considering the (first-order) spatiotemporal overlap between the adapting and test patterns. It should be noted in passing that the term "second- order" is used loosely in the literature. Many second-order stimuli do contain imbalances in first-order motion energy.

Nishida and Sato [4] used a $2f + 3f$ stimulus that was stepped $\frac{1}{4}$ of a cycle of the f grating at time intervals T. They analyzed the structure of this stimulus in terms of first- and second-order motion. By contrast, we find it more helpful to analyze the spatiotemporal structure of this stimulus in the usual Fourier space, followed by consideration in a velocity space. Stepping the $2f + 3f$ stimulus to the right at temporal intervals of T constitutes temporal sampling (at intervals 0, ,T, $2T$ etc) followed by convolution with a box function (see Appendix). This operation has the effect of replicating the Fourier spectrum at integer intervals of $\frac{1}{T} \equiv \gamma$. Consequently, the first few Fourier components of their stimulus are a $3f$ component moving to the left at $-\frac{1}{4}\gamma$ Hz, a $2f$ grating counterphasing at $\frac{1}{2}\gamma$ Hz, and a $3f$ grating moving to the right at $\frac{3}{4}\gamma$ Hz. In their experiment, the value of T ranged from 15 to 120 milliseconds, which induced changes in both the perceived direction of movement, and the resultant MAE durations. Changing T corresponds to changing γ, meaning that different components of the Fourier spectrum should become more or less influential. We find that these changes in the spatiotemporal structure of the adapting stimulus, considered in the usual velocity space, qualitatively predict both the changes in perceived direction and in the MAE durations.

Furthermore, experiments on velocity aftereffects find that shifts in perceived velocity following adaptation to either first- or second-order motion are very similar [29]. Such velocity aftereffects are briefly discussed in a later section (see Supporting Evidence).

Temporal Tuning

Whether static and flicker MAE strengths depend on the temporal frequency or velocity of the adapting stimulus is not entirely resolved. Pantle [30], using both duration and magnitude estimation techniques, found that the optimal static MAE was determined by temporal frequency rather than velocity. Using a cancellation method, Wright and Johnston [31] found that the maximum static MAE occured with an adapting grating between 6-10 Hz, regardless of spatial frequency. Using MAE duration as a measure, Ashida and Osaka [2] reported temporal frequency tuning for the static MAE, whereas in contrast, the flicker MAE showed a certain amount of velocity tuning. Regarding this question, the data of Bex et al. [26] were mixed: MAE duration showed a clear dependence on neither temporal frequency nor velocity.

Despite the mixed nature of the results described above, one aspect of the Wright and Johnston [31] data is worthy of remark. Specifically, at a fixed adapting temporal frequency, the required cancellation velocity (when testing a static MAE) was independent of spatial frequency. That is, adaptation at a fixed temporal frequency induced the same shift in *velocity* regardless of spatial frequency. This velocity constancy suggests that static MAEs could also be viewed in the context of velocity aftereffects, which we now discuss.

Supporting Evidence

This section is devoted to a brief summary of other evidence that supports the current proposal. At the beginning of the paper, we compared the spatiotemporal structure of the static and flicker tests. There, we pointed out that the static test can be viewed as a special case of a flicker test, where the test temporal frequency $\omega_{test} = 0$. It is also possible to investigate the effects of adaptation by measuring post-adaptation changes in perceived velocity [32, 33]. In such an experiment, following the usual adaptation period, subjects are required to provide velocity judgments of a grating moving at some test velocity v_{test}. Post-adaptation changes in perceived velocity are known as *velocity aftereffects*. Note that the static MAE can also be viewed as a special case in this context, where the test velocity $v_{test} = 0$.

Measuring such effects with a matching technique, Thompson [32] found a form of velocity constancy, in that adaptation stimuli of equal velocity (but different spatial and temporal frequencies) yielded similar patterns of aftereffects. If either spatial or temporal frequency alone were held constant, then the resultant pattern of aftereffects were different. As Thompson [32] noted, these results can be taken as evidence for the role of velocity channels, as we have proposed in this paper.

Ledgeway and Smith [29] measured velocity aftereffects following adaptation to first-order (FO) and second-order (SO) motion stimuli. The first-order stimuli were standard luminance sine wave gratings, whereas the second-order stimuli were contrast-modulated static noise patterns. Testing all four possible combinations of adapting and test stimuli, they showed changes in perceived speed for both same (FO/FO, SO/SO) and cross (SO/FO, FO/SO) adaptation conditions. When all motion stimuli were equated for visibility, the changes in perceived velocity were very similar. This similarity supports our approach of inferring a common substrate for the static and flicker MAEs induced by first- and second-order motion stimuli.

Schrater and Simoncelli [34] investigated shifts in perceived velocity (both speed and direction) following adaptation. After adapting to a single grating, they found that changes in the perceived motion direction of a plaid stimulus followed a shift in the plaid pattern motion, and not a shift in the motion of the plaid components. Furthermore, they showed that adapting to a random dot pattern induces velocity shifts that, in a two-dimensional velocity space (both speed and direction), tend to radiate away from the adapted location. These results support the role of mechanisms encoding two-dimensional pattern velocities in motion aftereffects.

Nishida et al. [13] investigated the dependence of static and flicker MAE durations on test and adaptation contrast. They found that the dependence for both types of aftereffect could be described by a function of adaptation contrast scaled by test contrast on a log axis. As they noted, this result suggests a functional similarity between the static and flicker MAEs.

Conclusions

The first contribution of this paper was to demonstrate a novel dissociation between the static and flicker MAEs. Specifically, we showed a number of first-order stimuli that produce a robust flicker MAE with little or no static MAE, as well as a stimulus with the opposite effect: it generates a moderate static MAE with little or no flicker MAE. On the basis of such dissociations, previous authors have proposed that flicker and static MAEs stem from anatomically distinct sites of adaptation in the visual system [2, 3, 5]. Contrary to this reasoning, we showed that it is not necessary to assume multiple sites of adaptation. Instead, this pattern of results is consistent with adaptation in an array of velocity-tuned units. The choice of velocity accounts for the important features of the experimental data: namely, interactions across relatively large spatial frequency differences, as well as the asymmetry in these interactions. Herein lies the second contribution of this paper: it supports the role of velocity mechanisms in motion adaptation.

We have emphasized that predicting the effects of adaptation requires consideration of the spatiotemporal structure of the adapting stimulus *as well as* the test stimulus. According to the current proposal, the occurrence of an aftereffect depends on the overlap between the adapted units, and those stimulated by the test pattern. In short, we have found that many of the reported differences between static and flicker MAEs could arise because the two tests probe a different set of velocity-tuned units. Such reasoning accounts for not only the results of the current experiments, but is also consistent with other differences between the static and flicker MAEs, including storage asymmetries [5], effects of temporal sampling [4], and differences in spatial frequency selectivity [6, 1].

In this paper, our focus has been on unifying the static and flicker MAEs within a framework of velocity-tuned cells. However, adaptation to moving stimuli can be measured in other ways, including the velocity aftereffect [32, 33] briefly discussed above, and the full-field flicker aftereffect reported by Green et al. [35]. Although in this paper we considered only one-dimensional stimuli, it is natural to consider adaptation in a two-dimensional space of *velocity*-tuned units. This higher dimensional space links to other known effects of motion adaptation, including changes in perceived direction of motion [36, 34]. The current approach encourages investigating all of these phenomena as different manifestations of the same underlying process.

References

[1] H. Ashida and N. Osaka. Difference of spatial frequency selectivity between static and flicker motion aftereffects. *Perception*, 23:1313–1320, 1994.

[2] H. Ashida and N. Osaka. Motion aftereffect with flickering test stimuli depends on adapting velocity. *Vision Research*, 35:1825–1834, 1995.

[3] S. Nishida, H. Ashida, and T. Sato. Complete interocular transfer of two types of motion aftereffect with flickering test. *Vision Research*, 34:2707–2716, 1994.

[4] S. Nishida and T. Sato. Motion aftereffect with flickering test pattern reveals higher stages of motion processing. *Vision Research*, 35:477–490, 1995.

[5] F.A.J. Verstraten, R.J. Fredericksen, R.J.A. van Wezel, R.J.A. Lankheet, and W.A. van de Grind. Recovery from adaptation for dynamic and static motion aftereffects: Evidence for two mechanisms. *Vision Research*, 36:421–424, 1996.

[6] E.L. Cameron, C.L. Baker, Jr., and J.C. Boulton. Spatial frequency selective mechanisms underlying the motion aftereffect. *Vision Research*, 32:561–568, 1992.

[7] D.H. Kelly. Fourier components of moving gratings. *Behavior Research Methods and Instrumentation*, 14:435–437l, 1982.

[8] V. Di Lollo and W. Bischof. Displacement limit (d max) of sampled directional motion: Direct and indirect estimates. *Perception and Psychophysics*, 49:176–186, 1991.

[9] C. Blakemore and F.W. Campbell. On the existence of neurones in the human visual system selectively sensitive to the orientation and size of retinal images. *Journal of Physiology*, 203:237–260, 1969.

[10] K.K. de Valois. Spatial frequency adaptation can enhance contrast sensitivity. *Vision Research*, 17:1057–1065, 1977.

[11] G.E. Legge and J.M. Foley. Contrast masking of human vision. *Journal of the Optical Society of America*, 70:1458–1471, 1980.

[12] C.F. Stromeyer and B. Julesz. Spatial-frequency masking in vision: Critical bands and spread of masking. *Journal of the Optical Society of America*, 62:1221–1232, 1972.

[13] S. Nishida, H. Ashida, and T. Sato. Contrast dependencies of two types of motion aftereffect. *Vision Research*, 37:553–563, 1997.

[14] E.H. Adelson and J.R. Bergen. Spatiotemporal energy models for the perception of motion. *Journal of the Optical Society of America*, A 2:284–299, 1985.

[15] D.J. Heeger. Model for the extraction of image flow. *Journal of the Optical Society of America*, A 4,:1455–1471, 1987.

[16] N.M. Grzywacz and A.L. Yuille. A model for the estimate of local image velocity by cells in the visual cortex. *Proceedings of the Royal Society of London*, B 239:129–161, 1990.

[17] E.P. Simoncelli and D.J. Heeger. A model of neuronal responses in visual area mt. *Vision Research*, 38:743–761, 1998.

[18] H.R. Rodman and T.D. Albright. Coding of visual stimulus velocity in area MT of the macaque. *Vision Research*, 27:2035–2048, 1987.

[19] N.S. Sutherland. Figural after-effects and apparent size. *Quarterly Journal of Experimental Psychology*, 13:222–228, 1961.

[20] G. Mather. The movement aftereffect and a distribution-shift model for coding the direction of visual movement. *Perception*, 9:379–382, 1980.

[21] H.B. Barlow and R.M. Hill. Evidence for a physiological explanation of the waterfall illusion and figural aftereffects. *Nature (London)*, 200:1345–1347, 1963.

[22] P. Hammond, G.S.V. Mouat, and A.T. Smith. Motion aftereffects in cat striate cortex elicited by moving texture. *Vision Research*, 26:1055–1060, 1986.

[23] M. Keck and B. Pentz. Recovery from adaptation to moving gratings. *Perception*, 6:719–725, 1977.

[24] M.J. Keck and T.D. Palella. Motion aftereffect as a function of the contrast of sinusoidal gratings. *Vision Research*, 16:187–191, 1976.

[25] R. Over, J. Broerse, B. Crassini, and W. Lovegrove. Spatial determinants of the aftereffect of seen motion. *Vision Research*, 13:1681–1690, 1973.

[26] P.J. Bex, F.J. Verstraten, and I. Mareschal. Temporal and spatial frequency tuning of the flicker motion aftereffect. *Vision Research*, 36:2721–2727, 1996.

[27] P. Thompson. The coding of velocity of movement in the human visual system. *Vision Research*, 24:41–45, 1984.

[28] N. Graham. Spatial frequency channels in the human visual system: effects of luminance and pattern drift rate. *Vision Research*, 12:53–68, 1972.

[29] T. Ledgeway and A.T. Smith. Changes in perceived speed following adaptation to first-order and second-order motion. *Vision Research*, 37:215–224, 1997.

[30] A. Pantle. Motion aftereffect magnitude as a measure of spatiotemporal response properties of direction sensitive analyzers. *Vision Research*, 14:1229–1236, 1974.

[31] M.J. Wright and A. Johnston. Invariant tuning of motion aftereffect. *Vision Research*, 25:1947–1955, 1985.

[32] P. Thompson. Velocity aftereffects: the effects of adaptation to moving stimuli on the perception of subsequently seen moving stimuli. *Vision Research*, 21:337–345, 1981.

[33] A.T. Smith. Velocity coding: Evidence from perceived velocity shifts. *Vision Research*, 25:1969–1976, 1985.

[34] P.R. Schrater and E.P. Simoncelli. Local velocity representation: Evidence from motion adaptation. 1998.

[35] M. Green, M. Chilcoat, and C.F. Stromeyer. Rapid motion aftereffect seen within uniform flickering test fields. *Nature*, 304:61–62, 1983.

[36] E. Levinson and R. Sekuler. Adaptation alters perceived direction of motion. *Vision Research*, 16:779–781, 1976.

[37] J.W. Goodman. *Introduction to Fourier Optics.* McGraw Hill Book Company, New York, 1968.

Appendix

In this appendix, we derive the Fourier amplitude spectra of the Wedge and Grids stimuli.

Wedge Stimulus

Spatial sampling can be described by the appropriate combination of the *Comb* and *Rect* functions, defined as follows:

$$Comb(ax) = \begin{cases} 1 & \text{if } ax \text{ is an integer} \\ 0 & \text{otherwise} \end{cases}$$

$$Rect(ax) = \begin{cases} 1 & \text{if } |x| \leq \frac{1}{2a} \\ 0 & \text{otherwise} \end{cases}$$

where the parameter a is the sampling density. The Wedge stimulus consists of moving sine wave grating sampled in space. In space-time, this operation is represented by a multiplication with the comb function in space, followed by convolution with a box car (*Rect*) function in space:

$$W(x,t) = [S(x,t) \times Comb(ax)] * Rect(ax) \tag{4}$$

where $S(x,t)$ is the usual travelling sine wave (see equation 1), and $*$ represents convolution in space.

Applying the Fourier transform to equation 4 yields:

$$\tilde{W}(f_x,\omega_t) = \left\{ \tilde{S}(f_x,\omega_t) * \frac{1}{a} Comb(\frac{f_x}{a}) \right\} \times \frac{1}{\pi f_x} \sin(\frac{\pi f_x}{a}) \tag{5}$$

Note that in the Fourier domain, the *Comb* function transforms to another *Comb* function [37]. Thus, it has the effect of replicating $\tilde{S}(f_x,\omega_t)$ — the Fourier spectrum of $S(x,t)$ (see Figure 1) — at integer intervals of the sampling parameter a. In the Wedge stimulus used in the current experiments, the sampling parameter $a = 8\, f_{fund}$, where f_{fund} is the fundamental frequency. Thus, the two point amplitude spectrum $\tilde{S}$ was replicated at $0f$, $\pm 8f$, $\pm 16f$ etc. The *Rect* function transforms to the *sinc* function [37], causing the absolute value of these replicated coefficients to decrease as $\frac{1}{f_x}$. Overall, the first three components of the amplitude spectrum are shown in Figure 10.

Grids Stimulus

The Grids stimulus consists of the usual travelling sine wave $S(x,t)$, punctuated by black grid lines. In space-time, this operation can be represented as follows:

$$G(x,t) = S(x,t)\,[Comb(ax) * Rect(bx)] \tag{6}$$

As before, this equation can be re-written in the Fourier domain:

$$\tilde{G}(f_x,\omega_t) = \tilde{S}(f_x,\omega_t) * \left\{ \frac{1}{a} Comb(\frac{f_x}{a}) \times \frac{1}{\pi f_x} \sin(\pi \frac{f_x}{b}) \right\} \tag{7}$$

With $a = 8 f_{fund}$, the sinusoidal spectrum $\tilde{S}$ is replicated at $0f$, $\pm 8f$, $\pm 16f$ etc., leaving a Fourier amplitude spectrum similar to that of Wedge pictured in Figure 10.

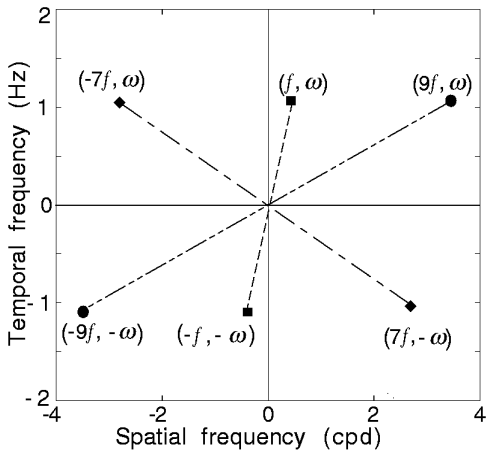

Figure 10: Part of the Fourier amplitude spectrum of the Wedge stimulus, created by covolution of a *Comb* function with the two- point spectrum of a moving sine wave grating. The two- point spectrum is replicated about integer multiples of the sampling parameter a, where in this cases $a = 8\, f_{fund}$.